Exploiting Ultra-Low Loss Silicon Nitride Platform for Various Applications (Invited)

Xingchen Ji [1,2,*], Michal Lipson[1,*]
[1]*Department of Electrical Engineering, Columbia University, New York, NY 10027, USA.*
[2]*Currently at John Hopcroft Center for Computer Science, Shanghai Jiao Tong University, Shanghai 200240, China*
[*]*xj53@cornell, ml3745@columbia.edu*

Abstract: Si_3N_4 has attracted extensive interest because of its wide applications in the field of biophotonics, telecommunications, nonlinear optics, and sensing. Here, we focus on exploiting ultra-low loss Si_3N_4 for on-chip delay line and frequency comb generation. © 2022 The Author(s)

Photonics uses light rather than electrons to perform a wide variety of applications. Silicon photonics, in particular, has gained a lot of interest in the past few decades due to its unique ability to utilize standard complementary metal-oxide-semiconductor manufacturing processes and materials, resulting in high density, high yield, and the massive fabrication of optical devices at low cost. Although the field has its roots in the telecommunications industry, it has expanded to many new applications such as sensing, spectroscopy, nonlinear optics, quantum optics, optomechanics, and even neuroscience. Silicon nitride (Si_3N_4), one of the mature silicon family materials has been widely used in photonics research and development. It combines the beneficial properties of a wide transparency range covering visible to mid-IR, a moderately high nonlinear refractive index ($n_2=2.4\times10^{-19}$ m^2/W) which is ten times higher than silica, and semiconductor mass manufacturing compatibility [1–3]. Most importantly, Si_3N_4 can achieve ultra-low loss and high confinement simultaneously.

The on-chip tunable photonic delay line is an application that significantly benefits from achieving ultra-low loss and high confinement at the same time. An on-chip tunable photonic delay line is a key building block for applications including sensing, imaging, and optical communication. However, it is still challenging to realize long and tunable photonic delay lines that are broad bandwidth within a small footprint. Here, we overcome this challenge by using ultra-low loss and high confinement Si_3N_4 waveguides with integrated microheaters [4]. We fabricate a 0.4 m long Si_3N_4 waveguide in an area of 8 mm^2 using 720 bends, each with a bending radius of only 80 µm. By integrating microheaters, we further use the thermo-optic effect of Si_3N_4 to enable tunability. We design the waveguides to ensure high thermal overlap between the optical mode and microheaters, while minimizing the loss from the metallic heaters (shown in Fig. 1).

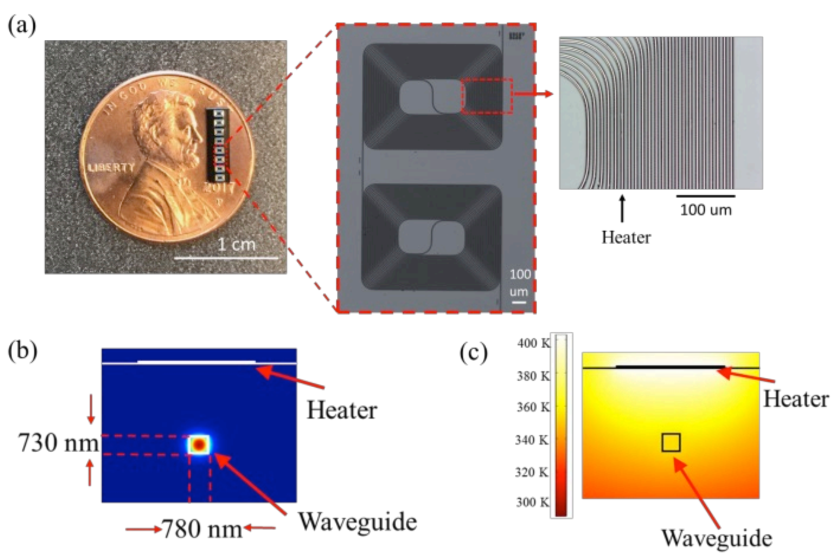

Fig. 1. (a) Fabricated 0.4 m long high confinement Si_3N_4 waveguide with an integrated platinum heater. (b) Mode simulation shows that the optical mode is not affected by the heater which ensures minimum losses. (c) Heat dissipation profile simulation for the integrated microheaters.

We measure the propagation loss to be 0.17 ± 0.01 dB/cm and show that the propagation loss has a linear dependence with the waveguide length, which indicates that the additional loss due to the misalignment is negligible in Fig. 2(a). We show the measured waveguide loss vs tuning range in Fig. 2(b). One can see that the waveguide tuning does not affect the loss. The measured waveguide loss vs wavelength is shown in Fig. 2(c). One can see that the waveguide loss does not change with wavelengths, which indicates that our delay line is broadband. With our 0.4 m long delay line chip, we have measured that the power conversion from TE to TM is only around 1%. So, the polarization state is well preserved in these long delay lines.

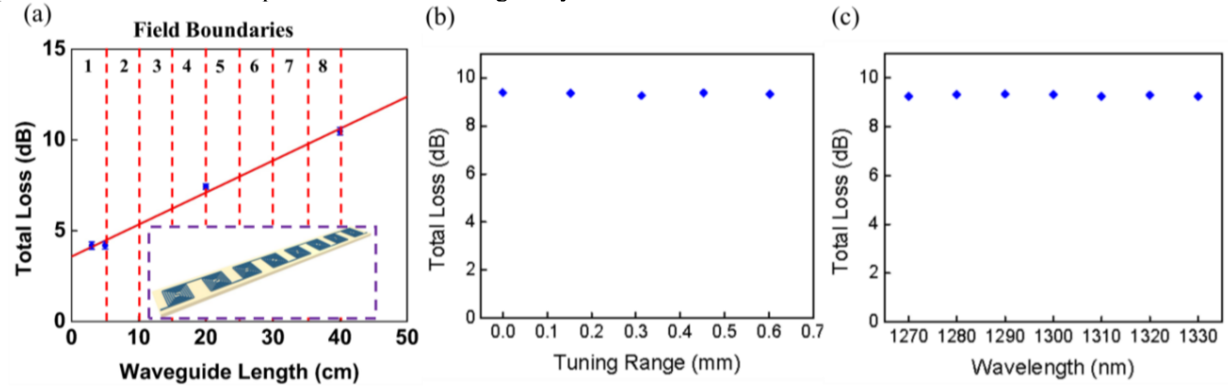

Fig. 2. (a) Measured loss of waveguides fabricated across different numbers of fields; the inset shows the schematic of the on-chip photonic delay line. We extract the propagation loss to be 0.17 ± 0.01 dB/cm. (b) Measured loss vs tuning ranges, the tuning does not affect the loss. (c) Measured loss vs different wavelengths, the waveguide loss does not change with wavelengths which indicates that our delay line is broadband.

We further show that the photonic delay line can enhance the capabilities of an optical coherence tomography (OCT) system. OCT is a non-invasive imaging modality that provides depth-resolved, high-resolution images of tissue microstructures in real-time and is an example of a technique that can significantly benefit from such an on-chip tunable delay line [5]. This is due to the fact that these high contrast OCT signals rely on zero-order interference, where the interferogram features the lowest possible spatial frequencies and its visibility can be maximized under quantized detection [6]. To demonstrate the capability of the on-chip tunable delay line, we couple it into a commercial spectrum domain (SD)-OCT system (Thorlabs Telesto I) around 1.3 μm to compensate the path length difference with a small footprint by replacing the reference arm in the system. We show that the delay line can extend the imaging range of OCT by 0.6 mm while maintaining a high signal-to-noise ratio (SNR). In Fig. 3, we show OCT B-scans taken from the endocardium side of the tissue before and after delay line tuning. The surface at the lower part of the OCT B-scan suffers from a reduced SNR (shown in Fig. 3a with zoom-in views shown in the red box) due to the fall-off of the SD-OCT system despite the use of a low-NA objective which ensures the surface remains within the depth of focus. In Fig. 3b one can see that after delay line tuning, the SNR of the surface area with the lower part of the OCT scan is increased. The tuning resolution is determined by the minimal incremental voltage applied to the heater. With an output voltage resolution of 1 mV, the tuning resolution of the delay line is 3 nm. The upper limit bandwidth of our 0.4 m long tunable photonic delay line is 229 GHz at 1.3 μm. Our tunable photonic delay line here is achieved without any moving parts which could provide high stability. This high stability is crucial for any interferometric measurements and, therefore, could benefit applications such as light detection and ranging (LIDAR), sensing, and coherent communication systems.

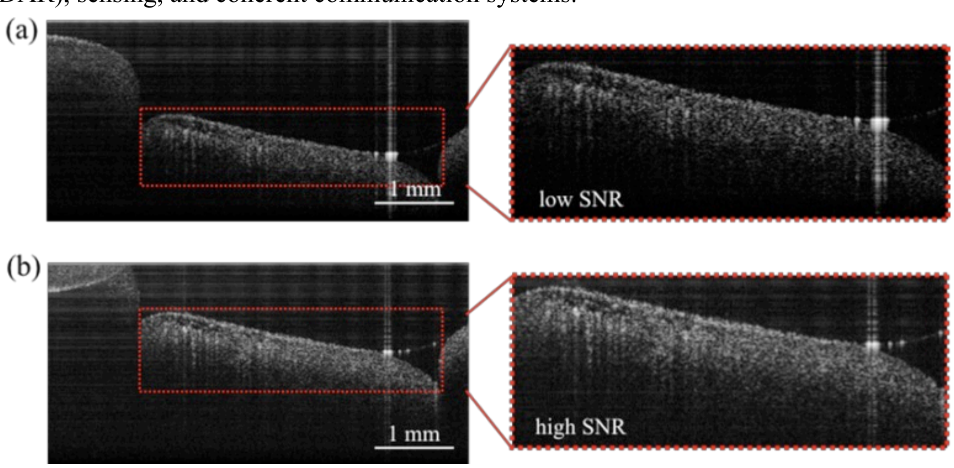

Fig. 3. High-topology, high-SNR OCT imaging of a human right ventricle sample from the endocardium side. Two images (a) and (b), taken before and after delay line tuning. Zoom-in views are shown in the red box, one can see that the SNR of the surface area with the lower part of the OCT scan is increased after the tuning.

Frequency comb generation is another application that greatly benefited from these ultra-low loss chip-scale devices. Because light can be tightly confined inside these devices for many roundtrips, nonlinear effects can be strongly enhanced. In recent years, there has been progress in the development of microresonator-based Kerr frequency comb, these frequency combs have triggered numerous applications, including in atomic clocks, optical communications, dual-comb spectroscopy, frequency synthesizers, and sensing. However, high pump powers are typically required to generate these frequency combs due to the high propagation losses, which hinders their usage in real-world applications. Sophisticated fabrication processes which yield sub-nm roughness have been developed to reduce scattering points at the waveguide interfaces in order to achieve ultralow propagation loss. Recently, we show ultralow propagation loss can be achieved by shaping the mode using a highly multimode structure to reduce its overlap with the waveguide interfaces, thus relaxing the fabrication processing requirements [7]. We use a novel design to minimize the interaction between the fundamental mode and excited higher-order modes in a highly multimode microresonator while achieving propagation loss <1 dB/m. We measure a record-low pump power threshold of 73 μW for parametric oscillation using the highly multimode microresonator and generate a broadband, almost octave spanning single soliton frequency comb without any fingerprint of higher-order modes, spanning from 1097 nm to 2040 nm (126 THz) with an FSR of 174 GHz.

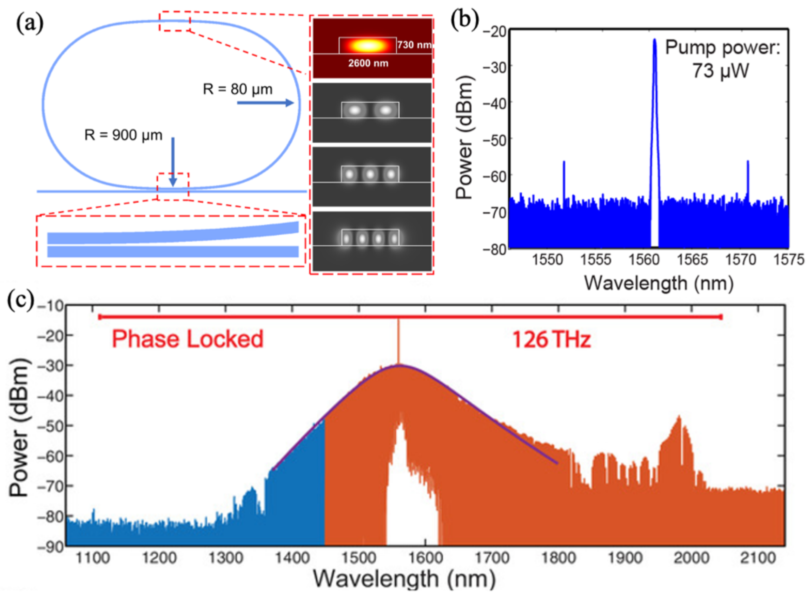

Fig. 4. (a) Schematic of microresonators with the novel adiabatic bends design. The bending radius is 900 μm in the coupling section and then gradually reduces to 80 μm in the sharpest bend. Inset shows the transverse electric (TE) modes supported by the waveguide and only the fundamental mode is excited in the adiabatic bends design. (b) Initial state of parametric oscillation was measured with a pump power of 73 μW. (c) A phase-locked single soliton frequency comb close to octave spanning. The broadband spectrum spans from 1097 to 2040 nm (126 THz) with an FSR of 174 GHz. The dips in the spectrum (at 1350 and 1850 nm for example) are due to the WDM filter, not due to mode crossings. The fit of a single soliton state with a spectral $sech^2$ envelope is shown in purple and it matches very well with our experimental result.

In summary, we discussed two application examples that significantly benefit from the ultra-low loss Si_3N_4 platform. Owing to the beneficial properties of Si_3N_4, we are expecting to see more applications that are enabled by the ultra-low loss Si_3N_4 platform in the future.

References

1. K. Ikeda, R. E. Saperstein, N. Alic, and Y. Fainman, "Thermal and Kerr nonlinear properties of plasma-deposited silicon nitride/silicon dioxide waveguides," Opt. Express, **16**, 12987–12994 (2008).
2. Y. Su, Y. Zhang, C. Qiu, X. Guo, and L. Sun, "Silicon Photonic Platform for Passive Waveguide Devices: Materials, Fabrication, and Applications," Advanced Materials Technologies **5**, 1901153 (2020).
3. X. Ji, S. Roberts, M. Corato-Zanarella, and M. Lipson, "Methods to achieve ultra-high quality factor silicon nitride resonators," APL Photonics **6**, 071101 (2021).
4. X. Ji, X. Yao, Y. Gan, A. Mohanty, M. A. Tadayon, C. P. Hendon, and M. Lipson, "On-chip tunable photonic delay line," APL Photonics **4**, 090803 (2019).
5. G. Yurtsever, B. Považay, A. Alex, B. Zabihian, W. Drexler, and R. Baets, "Photonic integrated Mach-Zehnder interferometer with an on-chip reference arm for optical coherence tomography," Biomed. Opt. Express, **5**, 1050–1061 (2014).
6. W. Drexler and J. G. Fujimoto " Optical Coherence Tomography: Technology and Applications," (Springer International Publishing, 2015).
7. X. Ji, J. K. Jang, U. D. Dave, M. Corato-Zanarella, C. Joshi, A. L. Gaeta, and M. Lipson, "Exploiting Ultralow Loss Multimode Waveguides for Broadband Frequency Combs," Laser & Photonics Reviews **15**, 2000353 (2021).